Synthesis of Zn, Mn doped Fe₃O₄ Nanoparticles with Tunable Size

CHENG Tian-Sheng[1,2,3], PAN Jiong[4], XU Ying-Ying[1,2,3], BAO Qun-Qun[1,2,3], HU Ping[1], SHI Jian-Lin[1]

(1. State Key Laboratory of High Performance Ceramics and Superfine Microstructures, Shanghai Institute of Ceramics, Chinese Academy of Sciences, Shanghai 200050, China; 2. University of Chinese Academy of Sciences, Beijing 100049, China; 3. Shanghai Tech University, Shanghai 201210, China; 4. Tongji University, Shanghai 200092, China)

Abstract: Zn, Mn doped Fe_3O_4 magnetic nanoparticles have broad application prospects in biomedicine for their excellent magnetic properties. Therein, the most remarkable property of magnetic nanoparticles is size-dependent biomagnetic applications, and size variation also affect their magnetic characteristics. Therefore, based on the specific requirements of size for various biological applications, it is critical to regulate their size. In this study, we synthesized 5–20 nm Zn, Mn doped Fe_3O_4 magnetic nanoparticles by changing reflux time duration, varying metal precursor and adding oil phase reducing agent (1,2-hexadecanediol). It is found that addition of 1,2-hexadecanediol is beneficial to the formation of smaller nanoparticles, while metal chloride and longer reflux time are helpful to prepare larger particles. Additionally, there exists a positive correlation between particle size and saturation magnetization.

Key words: Zn, Mn-Fe_3O_4 nanoparticles; size regulation; magnetic characteristics

Magnetic iron oxide nanoparticles (MNPs) have been researched extensively due to their promising applications for biomedicine such as hyperthermia[1-2], magnetic resonance imaging[3-4] and biolabeling[5]. Magnetic characteristics is highly significant for successful application of MNPs in biomedicine/biotechnology[6]. Recent studies suggest that a metal (Mn, Zn) dopant substitution strategy can achieve high magnetic performance[7-8]. The Zn, Mn doping level, a key factor, can be regulated by simply adjusting the original molar ratio of metal precursors. Moreover, when the ratio of doping Zn and Mn is 2:3, saturation magnetization (M_s) can reach its maximum[9].

For decades, a variety of preparation methods of MNPs achieved in hydrolytic phase have been developed, including hydrothermal reaction[10], Sol-Gel process[11] and coprecipitation method[12]. Magnetic iron oxide nanoparticles can also be obtained by organic-phase thermal decomposition of metal precursor, for example, decomposition of $Fe(acac)_2$ followed by oxidation to Fe_3O_4 in the presence of oleylamine and oleic acid[6,13]. Recent studies showed that organic-phase thermal decomposition methods could overcome the shortcomings of traditional hydrolytic one: it allows more strict control on particles uniformity and structure[14-15].

Size-dependent biomagnetic applications are the most remarkable properties of MNPs[16-17]. Different biological applications have specific requirements on particle size. For example, in the separation of cells, the size of MNPs should be 8 to 10 nm[17-18], but magnetothermal therapy requires larger nanoparticles, resulting from their higher specific absorption rate[19-20]. On the other hand, the size variation also affects the coercivity (H_c) and saturation magnetization (M_s) of the magnetic nanoparticles. However, it remains a great challenge to control MNPs size due to the lack of sufficient understanding of formation mechanism of magnetic particles referring to nucleation and growth process[21]. Therefore, it is necessary to study the effects of related parameters on particle size so that we can synthesize magnetic particle with tunable size. In this study, we present a one-step preparation of 5–20 nm Zn, Mn doped Fe_3O_4 (ZnMn-Fe_3O_4) nanoparticles, which can adapt to broader biomagnetic applications.

1 Experimental

Material Oleic acid (OAc) and Oleylamin (OAm) were purchased from Sigma-Aldrich. Other chemicals were purchased from Shanghai Aladdin Biochemical Technology Co. Ltd.

Preparation of 5 nm ZnMn-Fe₃O₄ nanoparticles Oleylamine (3 mmol), oleic acid (3 mmol), $Fe(acac)_3$ (1 mmol), $Zn(acac)_2$ (0.2 mmol) , $Mn(acac)_2$ (0.3 mmol)

and 1,2-hexadecanediol (5 mmol) were placed in a 50 mL three-neck round-bottom flask in the presence of 15 mL benzyl ether. The mixture was heated to 200 ℃ for 30 min and then to 300 ℃ for 1 h under argon atmosphere. After cooling to room temperature, excess ethanol was added to the solution, then a black powder precipitated and was collected by centrifugation. The magnetic nanoparticles were redispersed in cyclohexane.

Preparation of 10 nm ZnMn-Fe₃O₄ nanoparticles Oleylamine (3 mmol), oleic acid (3 mmol), $Fe(acac)_3$ (1 mmol), $Zn(acac)_2$ (0.2 mmol) and $Mn(acac)_2$ (0.3 mmol) were placed in a 50 mL three-neck round-bottom flask in the presence of 15 mL benzyl ether. The mixture was heated to 200 ℃ for 30 min and then to 300 ℃ for 1 h under argon atmosphere. After cooling to room temperature, excess ethanol was added to the solution, then a black powder precipitated and was collected by centrifugation. The magnetic nanoparticles were redispersed in cyclohexane.

Preparation of 15 nm ZnMn-Fe₃O₄ nanoparticles Oleylamine (3 mmol), oleic acid (3 mmol), $Fe(acac)_3$ (1 mmol), $ZnCl_2$ (0.2 mmol) and $MnCl_2$ (0.3 mmol) were placed in a 50 mL three-neck round-bottom flask in the presence of 15 mL benzyl ether. The mixture was heated to 200 ℃ for 30 min and then to 300 ℃ for 1 h under the atmosphere of argon. After cooling to room temperature, excess ethanol was added to the solution. The black precipitate was collected by centrifugation and washed with ethanol prior to redispersion in cyclohexane for further use. Similarly, by prolonging reaction time to 1.5 or 2 h, 20 nm ZnMn-Fe₃O₄ nanoparticles can be prepared.

Characterization Transmission electron microscopy (TEM) was performed on JEM-2100F instruments. The XRD studies were conducted *via* a Rigaku D/MAX-2250V diffractometer with a Cu Kα radiation source (40 kV, 120 Ma). Magnetic measurements were performed on a Vibrating Sample Magnetometer (VSM). FT-IR spectra were recorded by an IRPRESTIGE-21 spectrometer (Shimadzu) using KBr pellets. Size distribution were measured on Nano-Zetasizer (Malvern Instruments Ltd.).

2 Results and discussion

Reductive effect As shown in Fig. 1(a), monodispersed ZnMn-Fe₃O₄ nanoparticles about 5 nm were fabricated by decomposition of $Fe(acac)_2$, $Mn(acac)_2$ and $Zn(acac)_2$ in the presence of oleylamine, oleic acid and 1,2-hexadecanediol. Under the same experimental conditions, if 1,2-hexadecanediol was not added, the size of particles increased from 5 nm to 10 nm (Fig. 1(b)), which were further proved by the alteration of size distribution
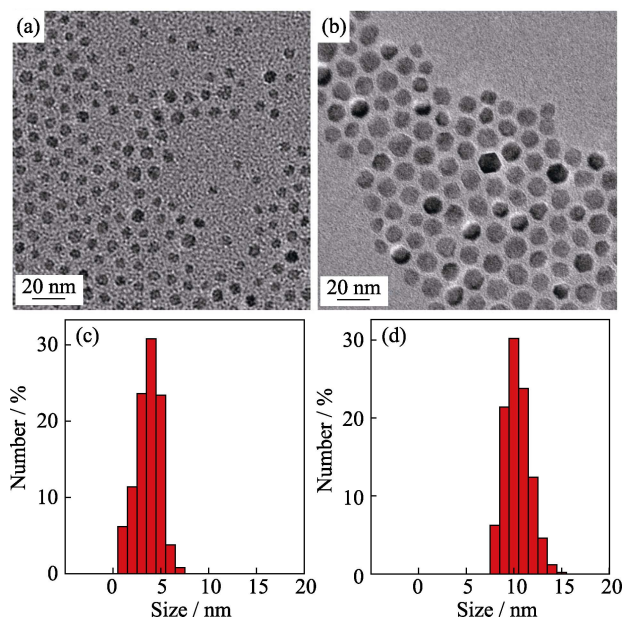

Fig. 1 TEM images of ZnMn-Fe₃O₄ nanoparticles and histograms of their size distributions obtained by $Fe(acac)_3$, $Mn(acac)_2$ and $Zn(acac)_2$ with (a, c) and without (b, d) adding 1,2-hexadecanediol

(Fig. 1(c, d)). Organic-phase thermal decomposition in fact is a process that activates metal atoms to nucleate and grow[21-22], so the size of particles is mainly dependent on the nucleation and growth rate of metal atoms. Herein, the addition of strong reductive 1,2-hexadecanediol contributed to facile reduction of $M(acac)_2$ to M^0 (M=Zn, Mn), leading to faster consumption of metal acetylactone and nucleation of particles, as a result, smaller nanoparticles were formed.

Metal precursor effect Metal precursors play an important role in size regulation of magnetic nanoparticles. The size of nanoparticles synthesized by metal chloride as precursor is about 15 nm with narrow size distribution (Fig. 2(a, b)). The high resolution TEM (Fig. 2(c)) and selected area electron diffraction (SAED) pattern (Fig. 2(d)) suggest that the particles have high-quality crystallinity. In contrast, using acetylacetone as metal precursor, the size of obtained nanoparticles is about 10 nm (Fig. 1(b)). According to chemical bond theory, metal chloride is more stable than metal acetylacetone, thus it requires higher decomposition temperature. Therefore, the addition of metal chloride may lead to slower nucleation rate, more metal precursor could deposit surrounding the nuclei formed in mixture and resulting in larger nanoparticles.

Reflux time effect It is also important to study the effect of reaction time on the size of nanoparticles. In this work, we found that larger particles could be obtained by longer reflux time. As shown in Fig. 3(a), when reflux time was postponed from 1 h to 1.5 h under the same reaction condition, the particles size increased from
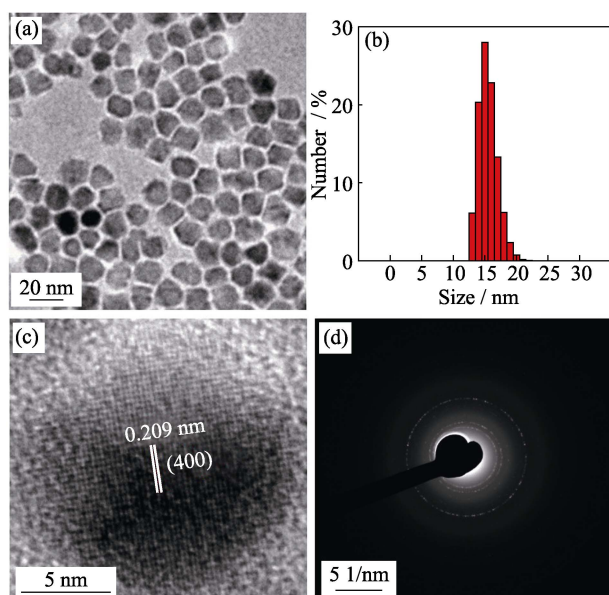
Fig. 2   TEM image (a), histograms of their size distributions (b), high-resolution TEM image (c) and selected area electron diffraction (SAED) pattern (d) of 15 nm-sized ZnMn-Fe$_3$O$_4$ nanoparticles prepared from Fe(acac)$_3$, MnCl$_2$ and ZnCl$_2$
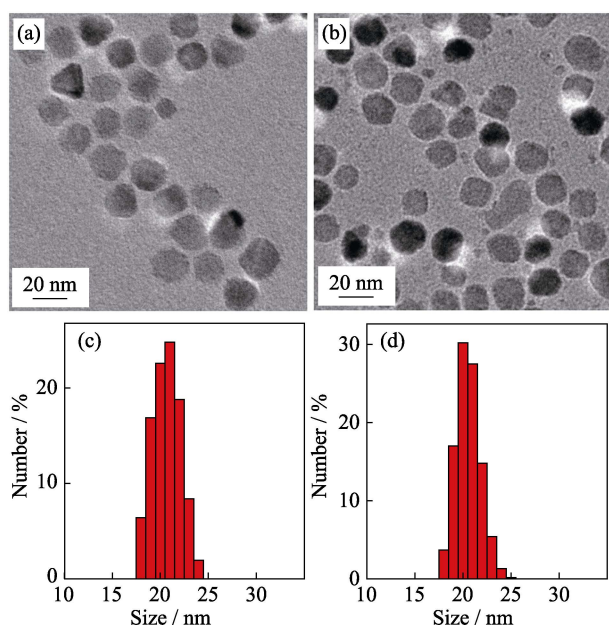
Fig. 3   TEM images of 20 nm-sized ZnMn-Fe$_3$O$_4$ nanoparticles synthesized from Fe(acac)$_3$, MnCl$_2$ and ZnCl$_2$ with different reflux time durations of 1.5 h (a) and 2 h (b), and the corresponding histograms of size distributions of 1.5 h (c) and 2 h (d)

15 nm (Fig. 2(a)) to 20 nm (Fig. 3(a)), which were further proved by the alteration of size distribution (Fig. 3(c)). However, further prolongation of the reflux time to 2 h resulted in no distinct increase in the size of nanoparticles (Fig. 3(b, d)), which indicates that the nanocrystals will stop growing when the reaction reaches homeostasis. In the meantime, it seems to produce new nanocrystal with longer reflux time (Fig. 3(b)).

The XRD pattern (Fig. 4(a)) shows a single-phase spinel structure of 5–20 nm ZnMn-Fe$_3$O$_4$ nanoparticles and the relative intensity and position of all diffraction peaks/rings accord well with previously reported Zn, Mn doped Fe$_3$O$_4$ powder[23], which indicates that crystal structure has little relevance with particle size. Two characteristic stretching were recorded in FT-IR spectrum at 2920 and 2850 cm^{-1}, 1630, and 1410 cm^{-1} corresponding to H–C–H, C–O stretching, respectively (Fig. 4(b)), which reveals that particles are coated by oleylamine and oleic acid. In this case, in addition to acting as reductive, oleylamine and oleic acid also work as surfactant. The organic surfactants can be removed by 2,3-dimercaptosuccinic acid (DMSA) to yield water-soluble nanoparticles[20]. The Zn, Mn doping levels were measured by energy dispersive X-ray spectroscopy (EDS) and the results indicate that 5–20 nm particles have similar element composition (Fig. 4(c)).

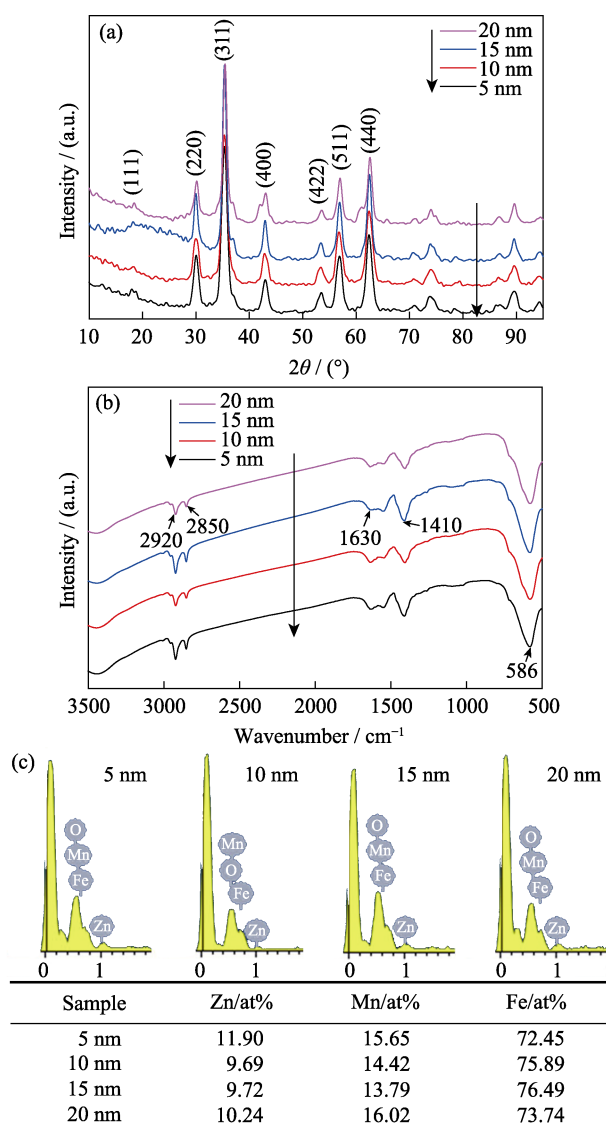| Sample	Zn/at%	Mn/at%	Fe/at%
5 nm	11.90	15.65	72.45
10 nm	9.69	14.42	75.89
15 nm	9.72	13.79	76.49
20 nm	10.24	16.02	73.74

Fig. 4   XRD patterns (a), FT-IR spectra (b) and energy dispersive X-ray spectroscopy (EDS) data (c) of 5 nm, 10 nm, 15 nm, and 20 nm-sized ZnMn-Fe$_3$O$_4$ nanoparticles
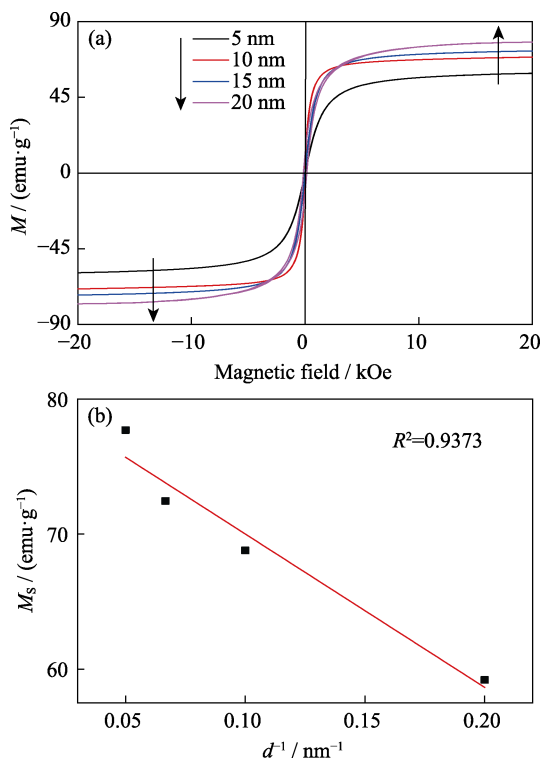
Fig. 5 Magnetic hysteresis curve (a) and d^{-1}-dependent M_s curve (b) of 5–20 nm-sized ZnMn-Fe$_3$O$_4$ nanoparticles

Size effect on magnetic characteristics Magnetic characteristics of MNPs with different size were measured by VSM at 300 K, and the results are shown in Fig. 5(a). The hysteresis curve of MNPs in 5–15 nm exhibits superparamagnetism without remnant magnetization. However, 20 nm particles are ferromagnetic with a coercivity of 150 Oe (1 Oe≈79.6 A/m). Saturation magnetization (M_s) value of MNPs gradually increased as the size of MNPs increased from 5 to 20 nm, and reached the maximum of 77.7 emu/g (emu/g=$4\pi \times 10^{-7}$ Wb·m/kg). As Fig. 5(b) shown, M_s and d^{-1} (the reciprocal of the nanoparticles size) display an approximate linear relationship, which is consistent with previous reports[24-25].

3 Conclusion

We have successfully synthesized 5–20 nm ZnMn-Fe$_3$O$_4$ by changing metal precursors, varying reflux time and adding 1,2-hexadecanediol. These ferrite nanoparticles with different particle sizes could adapt to the needs of extensive biomagnetic applications. Smaller sized nanoparticles could be obtained by introducing extra reducing power 1,2-hexadecanediol, and we can prepare larger particles by using more stable metal precursor and extending reflux time. These seem to indicate that powerful reducing agent and metal precursor with low decomposition temperature will yield smaller particles. Meanwhile, the magnetic characteristics of ZnMn-Fe$_3$O$_4$ are closely

related to particle size. Understanding how the different parameters impact on particle size is extremely critical to develop a more predictive and controllable way to synthesize the MNPs.

References:

[1] NOH S H, NA W, JANG J T, et al. Nanoscale magnetism control via surface and exchange anisotropy for optimized ferrimagnetic hysteresis. *Nano Letters*, 2012, **12(7):** 3716–3721.

[2] DI CORATO R, BEALLE G, KOLOSNJAJ-TABI J, et al. Combining magnetic hyperthermia and photodynamic therapy for tumor ablation with photoresponsive magnetic liposomes. *ACS Nano*, 2015, **9(3):** 2904–2916.

[3] NA H B, SONG I C, HYEON T. Inorganic nanoparticles for MRI contrast agents. *Advanced Materials*, 2009, **21(21):** 2133–2148.

[4] GAO J H, GU H W, XU B. Multifunctional magnetic nanoparticles: design, synthesis, and biomedical applications. *Accounts of Chemical Research*, 2009, **42(8):** 1097–1107.

[5] WAN Y, CHENG G, LIU X, et al. Rapid magnetic isolation of extracellular vesicles via lipid-based nanoprobes. *Nature Biomedical Engineering*, 2017, **1:** 0058.

[6] LU A H, SALABAS E L, SCHUTH F. Magnetic nanoparticles: synthesis, protection, functionalization, and application. *Angew. Chem. Int. Ed.*, 2007, **46(8):** 1222–1244.

[7] HOCHEPIED J F, PILENI M P. Magnetic properties of mixed cobalt-zinc ferrite nanoparticles. *Journal of Applied Physics*, 2000, **87(5):** 2472–2478.

[8] ARULMURUGAN R, JEYADEVAN B, VAIDYANATHAN G, et al. Effect of zinc substitution on Co-Zn and Mn-Zn ferrite nanoparticles prepared by co-pecipitation. *Journal of Magnetism and Magnetic Materials*, 2005, **288:** 470–477.

[9] JANG J T, NAH H, LEE J H, et al. Critical enhancements of MRI contrast and hyperthermic effects by dopant-controlled magnetic nanoparticles. *Angew. Chem. Int. Ed.*, 2009, **48(7):** 1234–1238.

[10] DENG H, LI X, PENG Q, et al. Monodisperse magnetic single-crystal ferrite microspheres. *Angew. Chem. Int. Ed.*, 2005, **44(18):** 2782–2785.

[11] WOO K, LEE H J, AHN J P, et al. Sol–Gel mediated synthesis of Fe$_2$O$_3$ nanorods. *Advanced Materials*, 2003, **15(20):** 1761–1764.

[12] WU J H, KO S P, LIU H L, et al. Sub 5 nm magnetite nanoparticles: synthesis, microstructure, and magnetic properties. *Materials Letters*, 2007, **61(14/15):** 3124–3129.

[13] XIE J, LEE S, CHEN X. Nanoparticle-based theranostic agents. *Advanced Drug Delivery Reviews*, 2010, **62(11):** 1064–1079.

[14] LEE J H, HUH Y M, JUN Y W, et al. Artificially engineered magnetic nanoparticles for ultra-sensitive molecular imaging. *Nature Medicine*, 2007, **13(1):** 95–99.

[15] SINGH M, RAMANATHAN R, MAYES E L H, et al. One-pot synthesis of maghemite nanocrystals across aqueous and organic solvents for magnetic hyperthermia. *Applied Materials Today*, 2018, **12:** 250–259.

[16] FORTIN J P, WILHELM C, SERVAIS J, et al. Size-sorted anionic iron oxide nanomagnets as colloidal mediators for magnetic hyperthermia. *Journal of the American Chemical Society*, 2007, **129(9):** 2628–2635.

[17] GU H, XU K, XU C, et al. Biofunctional magnetic nanoparticles for protein separation and pathogen detection. *Chem. Commun.*, **2006(9):** 941–949.

[18] XU H, AGUILAR Z P, YANG L, et al. Antibody conjugated mag-

netic iron oxide nanoparticles for cancer cell separation in fresh whole blood. *Biomaterials*, 2011, **32(36)**: 9758–9765.

[19] LEE J H, JANG J T, CHOI J S, *et al*. Exchange-coupled magnetic nanoparticles for efficient heat induction. *Nature Nanotechnology*, 2011, **6(7)**: 418–422.

[20] LARTIGUE L, INNOCENTI C, KALAIVANI T, *et al*. Water-dispersible sugar-coated iron oxide nanoparticles. An evaluation of their relaxometric and magnetic hyperthermia properties. *Journal of the American Chemical Society*, 2011, **133(27)**: 10459–10472.

[21] WU L, MENDOZA-GARCIA A, LI Q, *et al*. Organic phase syntheses of magnetic nanoparticles and their applications. *Chemical Reviews*, 2016, **116(18)**: 10473–10512.

[22] SUN S H, ZENG H, ROBINSON D B, *et al*. Monodisperse MFe₂O₄ (M = Fe, Co, Mn) nanoparticles. *Journal of the American Chemical Society*, 2004, **126(1)**: 273–279.

[23] QU Y, LI J, REN J, *et al*. Enhanced magnetic fluid hyperthermia by micellar magnetic nanoclusters composed of $Mn_{(x)}Zn_{(1-x)}Fe_{(2)}O_{(4)}$ nanoparticles for induced tumor cell apoptosis. *ACS Appl. Mater. Interfaces*, 2014, **6(19)**: 16867–16879.

[24] RONG C B, LI D, NANDWANA V, *et al*. Size-dependent chemical and magnetic ordering in L10-FePt nanoparticles. *Advanced Materials*, 2006, **18(22)**: 2984–2988.

[25] JUN Y W, HUH Y M, CHOI J S, *et al*. Nanoscale size effect of magnetic nanocrystals and their utilization for cancer diagnosis *via* magnetic resonance imaging. *Journal of the American Chemical Society*, 2005, **127(16)**: 5732–5733.

锌锰掺杂 Fe₃O₄ 纳米颗粒的尺寸可控合成

程田盛 [1,2,3]，潘　炯 [4]，徐鹰鹰 [1,2,3]，鲍群群 [1,2,3]，胡　萍 [1]，施剑林 [1]

(1. 中国科学院 上海硅酸盐研究所, 高性能陶瓷和超微结构国家重点实验室, 上海 200050; 2. 中国科学院大学, 北京 100049; 3. 上海科技大学, 上海 201210, 4. 同济大学, 上海 200092)

摘　要: 锌锰掺杂的 Fe₃O₄ 纳米颗粒具有优异的磁性能, 在生物医药领域有广泛的应用前景。磁性纳米颗粒的尺寸与其磁学性质以及生物磁性应用密切相关。因此, 为了适应不同生物应用对尺寸的需求, 研究其尺寸调控具有重要的意义。在本研究中, 我们采用高温热分解法, 通过加入还原剂 1,2-十六烷二醇, 改变金属前躯体和回流时间成功制备了尺寸在 5~20 nm 的锌锰掺杂 Fe₃O₄ 纳米颗粒。研究发现:强还原剂 1,2-十六烷二醇的加入有利于合成小尺寸的纳米颗粒, 而以金属氯化物作为金属前躯体和延长回流时间可以进一步合成更大尺寸的纳米颗粒; 纳米颗粒的饱和磁化强度随着尺寸的增大而增大。

关　键　词: 锌锰掺杂 Fe₃O₄ 纳米颗粒; 尺寸调控; 磁学性质

中图分类号: TQ174　　**文献标识码:** A